









Isolation, characterization, and encapsulation of a lupeol-rich fraction obtained from the hexanic extract of *Coccoloba uvifera* L. leaves

Carla N. Cruz-Salas¹ , Zoran Evtoski² , Montserrat Calderón-Santoyo¹ , José M. Lagarón² , Cristina Prieto^{2*} , Juan A. Ragazzo-Sánchez^{1*} 

¹Laboratorio Integral de Investigación en Alimentos, Tecnológico Nacional de México/Instituto Tecnológico de Tepic, Tepic, Nayarit 63175, México

²Novel Materials and Nanotechnology Group, Institute of Agrochemistry and Food Technology (IATA), Spanish Council for Scientific Research (CSIC), 46980 Paterna, Spain

***Correspondence:** Cristina Prieto, Novel Materials and Nanotechnology Group, Institute of Agrochemistry and Food Technology (IATA), Spanish Council for Scientific Research (CSIC), Calle Catedrático Agustín Escardino Benlloch 7, 46980 Paterna, Spain. cprieto@iata.csic.es; Juan A. Ragazzo-Sánchez, Laboratorio Integral de Investigación en Alimentos, Tecnológico Nacional de México/Instituto Tecnológico de Tepic, Avenida Tecnológico #2595, Colonia Lagos del Country, Tepic, Nayarit 63175, México. jragazzo@tepic.tecnm.mx

Academic Editor: Marcello Iriti, Milan State University, Italy

Received: April 22, 2023 **Accepted:** June 28, 2023 **Published:** August 28, 2023

Cite this article: Cruz-Salas CN, Evtoski Z, Calderón-Santoyo M, Lagarón JM, Prieto C, Ragazzo-Sánchez JA. Isolation, characterization, and encapsulation of a lupeol-rich fraction obtained from the hexanic extract of *Coccoloba uvifera* L. leaves. *Explor Foods Foodomics*. 2023;1:115–29. <https://doi.org/10.37349/eff.2023.00010>

Abstract

Aim: This study aimed to isolate, characterize, and encapsulate a lupeol-rich fraction obtained from the hexanic extract of *Coccoloba uvifera* L. leaves to evaluate its potential use in nutraceutical or pharmaceutical applications.

Methods: The *C. uvifera* leaf extract was fractionated by column chromatography and the presence of lupeol was assessed by thin layer chromatography, attenuated total reflection-Fourier transform infrared (ATR-FTIR) spectroscopy, nuclear magnetic resonance (NMR), and liquid chromatography-mass spectrometry (LC-MS). Additionally, the lupeol-rich fraction was characterized according to its antioxidant capacity and cytotoxicity. Finally, this fraction was encapsulated into electrospun nanofibers made of high degree of polymerization agave fructans (HDPAF) combined with polyethylene oxide (PEO). The obtained nanofibers were characterized in terms of morphology, chemical composition, and *in vitro* permeability using the Caco-2 cell line.

Results: Fraction 6 showed a 77% of lupeol, quantified by chromatography, and presented a 7.3% inhibition of 2,2-diphenyl-1-picrylhydrazyl (DPPH). 100 µg/mL of fraction 6 showed a decrease in Caco-2 cell viability. Finally, fraction 6 was encapsulated into electrospun nanofibers, which showed an increase in the apparent permeability of the lupeol present in fraction 6 in Caco-2 cells in comparison to neat fraction 6.

Conclusions: It was possible to isolate and encapsulate a lupeol-rich fraction from *C. uvifera* into electrospun nanofibers, which allows the increasing the apparent permeability of lupeol, and consequently, they could be used for nutraceutical or pharmaceutical applications.

© The Author(s) 2023. This is an Open Access article licensed under a Creative Commons Attribution 4.0 International License (<https://creativecommons.org/licenses/by/4.0/>), which permits unrestricted use, sharing, adaptation, distribution and reproduction in any medium or format, for any purpose, even commercially, as long as you give appropriate credit to the original author(s) and the source, provide a link to the Creative Commons license, and indicate if changes were made.



Keywords

Coccoloba uvifera leaves, lupeol-rich fraction, cytotoxicity, electrospinning, *in vitro* Caco-2 permeability

Introduction

Natural extracts present high content of high biological value compounds (HBVC), which are known for presenting gastroprotective, hepatoprotective, cytotoxic, anti-inflammatory, antitumor, and antiviral properties, among others [1–3]. This fact favors the interest in their isolation and purification for their application in the prevention and treatment of diseases [4].

Lupeol is a pentacyclic triterpene characterized by having biological properties such as antioxidant, antimicrobial, anti-inflammatory, anticancer, antimutagenic, antiproliferative, and gastroprotective properties, among others [2, 5, 6]. This compound is present in different plant families, such as olive fruit, ginseng oil, Japanese pear, elm plant, aloe, and mango [5, 7]. Recently, Ramos-Hernandez et al. (2019) [8] reported the presence of lupeol in *Coccoloba uvifera* L. trees, proving that *C. uvifera* leaves contained the highest concentration of lupeol, and confirmed that its extraction assisted by ultrasounds was the most efficient method to extract this compound [8]. Then, Cruz-Salas et al. (2022) [9] performed the characterization of this *C. uvifera* L. extract and studied its antimutagenic and antiproliferative activity, as well as performed its encapsulation in gelatin-agave fructans electrospun nanofibers. Therefore, it would be interesting to perform a more in depth study, isolating and purifying lupeol from *C. uvifera* extract, characterize its bioactive properties, as well as study its safety [10, 11].

Therefore, the aim of the present study was to isolate, purify, characterize and encapsulate lupeol obtained from the hexane extract of *C. uvifera* leaves to evaluate its potential use in nutraceutical or pharmaceutical applications. The isolation of lupeol from the extract was performed by column chromatography and lupeol was identified by thin-layer chromatography (TLC). The chemical and structural characterization of the lupeol-rich fraction was made by attenuated total reflection-Fourier transform infrared (ATR-FTIR) spectroscopy, nuclear magnetic resonance (NMR), and liquid chromatography coupled to mass spectrometry. The characterization of the antioxidant capacity and the cytotoxicity was performed. Finally, the lupeol-rich fraction was encapsulated into electrospun nanofibers made of high degree of polymerization agave fructans (HDPAF) combined with polyethylene oxide (PEO), and the obtained fibers were characterized in terms of morphology, chemical composition and apparent permeability using the Caco-2 cell line.

Materials and methods

Materials

Leaves of *C. uvifera* were collected at Tecolutla, Veracruz, Mexico and transferred to the Laboratorio Integral de Investigación en Alimentos (LIIA) of the Tecnológico Nacional de México (Tepic, Nayarit, México). They were washed and dried until reaching 5% humidity. Subsequently, they were ground and sieved (1 mm, pore size). A homogeneous green powder was obtained and stored in a desiccator at 25°C, until the extraction process.

N-hexane (Jalmek, Nuevo León, Mexico); ethyl acetate; resazurin sodium salt were purchased from MP Biomedicals, LLC. (Illkirch, France). 96° ethanol was obtained from Guinama (Spain). Caco-2 cell lines; Eagle's Minimum Essential Medium (EMEM); fetal bovine serum; trypsin-EDTA; were purchased from ATCC® (Manassas, VA, USA). Penicillin-streptomycin, amphotericin-B, lipopolysaccharides (LPS), lupeol standard, PEO (Mw of 400,000) and silica gel (60 Å, 40–63 µm) were obtained all from Sigma Aldrich® (St. Louis, MO, USA). The surfactant TEGO SML was obtained from Evonik Industries AG. (Germany). HDPAF were obtained in the LIIA of ITT. Deionized water was used throughout the study.

Lupeol extraction from *C. uvifera* leaves

The extraction conditions were optimized in previous works conducted by Ramos-Hernández et al. and Cruz-Salas et al. [8, 9]. To obtain the extract, the methodology reported by Cruz-Salas et al. (2022) [9] was

used. Briefly, the powdered plant material was mixed with n-hexane in a 1:10 ratio (w/v), and the mixture was sonicated at 42 kHz at 25°C for 30 min in a CD-4820 Kendal Digital Ultrasonic Cleaner (China) and vacuum filtered using Whatman™ 1 paper filters (110 mm, diameter). The solvent was removed on a rotary evaporator IKA RV10 (Wilmington, NC, USA) at 200 rpm at 45°C. The extract obtained was placed in an extraction hood to eliminate solvent residues and stored in a desiccator until further use.

Fractionation of the *C. uvifera* extract

The purification process for obtaining a lupeol-rich fraction was performed by column chromatography. A vertical chromatographic column 50 cm long and 1.5 cm of diameter was used. Silica gel was used as stationary phase and gradients of 100 mL hexane (100%), 200 mL hexane-ethyl acetate (95:5), 100 mL hexane-ethyl acetate (80:20) were used. The stationary phase was conditioned with 100 mL of hexane (100%), and then, the *C. uvifera* extract previously diluted (1:20 ratio) in hexane was added. The gradients were successively fed to the column, which facilitated the transfer of the compounds through the stationary phase, and an average volume of 1 mL of effluent per sample was continuously collected.

Qualitative identification of lupeol in fraction 6

A qualitative identification of the different fractions was carried out using the TLC technique, which has been previously used to identify fractions rich in lupeol from the hexane extract of *Solanum melongena* L [12]. Silica gel plates on TLC Al foils (20 cm × 20 cm, 60 Å medium pore diameter, Sigma-Aldrich®, Steinheim, Germany) were used as stationary phase, using the mixture of hexane, ethyl acetate and dichloromethane in ratio 80:10:10 respectively, as mobile phase. The identification of the fractions was carried out by placing on a plate the references of the standards of the compounds to be identified, the extract and the samples obtained from the elution. Samples with same signals on TLC were considered as the same fraction. Solvent was removed from the obtained fractions, and the resultant dried fractions were stored in sterile vials in a desiccator until further analysis.

Identification of lupeol in fraction 6 by ATR-FTIR spectroscopy

A Bruker Tensor 37 FT-IR spectrometer (Bruker, Ettlingen, Germany) coupled with the ATR sampling accessory Golden Gate™ (Specac Ltd., Orpington, UK) was used to compare the ATR-FTIR spectra of the lupeol-rich fraction and lupeol standard. All spectra were recorded between 4,000 and 600 cm⁻¹, with a resolution of 4 cm⁻¹, and averaging 10 scans. The software Opus 4.0 (Bruker, Ettlingen, Germany) was used to analyze the spectral data. Same methodology was used for the analysis of the electrospun fibers encapsulating the lupeol-rich fraction.

Identification of lupeol in fraction 6 by NMR

NMR analysis was performed using the high-resolution one-dimensional technique on a Bruker AVANCE III 400 MHz equipment (Bruker Corporation am Silberstreifen, Rheinstetten, Germany). 10 mg of the sample were dissolved in 0.5 mL of deuterated chloroform (CDCl₃) the mixture was filtered before being analyzed. Samples were analyzed in triplicates. Spectra were analyzed with Bruker TopSpin 3.2 software (Bruker Corporation am Silberstreifen, Rheinstetten, Germany).

Identification and quantification of lupeol in fraction 6 by liquid chromatography-mass spectrometry

A Waters® ACQUITY® TQD equipment (Milford, M.A, USA) with the multiple reaction monitoring (MRM) mode was used. 5 µL of the fraction was injected into the liquid chromatography-mass spectrometry (LC-MS) using the autosampler. A Luna® Omega polar® C18 UHPLC column, (1.6 µm; 100 × 2.1 mm) (Phenomenex) was used at 40°C. A flow of 0.4 mL/min was applied. The mobile phase consisted of a gradient of acidified water (0.1% formic acid): acetonitrile. The analysis was carried out by applying the gradient at different times: 35:65 (0 min), 95:05 (1.2 min), 35:65 (3.3 min), respectively. The lupeol standard was used to develop the calibration curve ($y = 1.8558x + 22.0701$, $r^2 = 0.9925$, where x is the concentration in ng/mL and y is the area under the curve) in the concentration range from 10 to 1,000 ng/mL with LOD: 0.8421 ng/mL and LOQ: 2.5518 ng/mL. Spectra were obtained with positive and

negative ionization, MRM mode and the transition of lupeol was 427.0 > 315.2, using Systems supported on MassLynx 4.1 or Empower 2 Software (Milford, MA, USA). Samples were analyzed in triplicates.

Determination of antioxidant capacity

Measurements were performed by dissolving 10 mg of extract in 1 mL of methanol, 50 μ L of the stock solution were taken and diluted with 950 μ L of methanol. 0.1 mL of solution were mixed with 1.9 mL of 2,2-diphenyl-1-picrylhydrazyl (DPPH) 0.094 mM in methanol and stored protected from the light for 30 min. The absorbance was read at 517 nm in a Cary 50-Bio UV-Vis spectrophotometer (Varian, Australia PTY). The DPPH radical inhibition was calculated using equation 1:

$$\text{DPPH inhibition (\%)} = (A - B) / A \times 100 \text{ (equation 1)}$$

Where A is the DPPH absorbance and B is the sample absorbance. Samples were analyzed in triplicates.

Cytotoxicity assay

Caco-2 cell culture

The study was carried out to determine the applicable range of non-toxic concentrations of fraction 6 using the human colon adenocarcinoma cell line (Caco-2), to perform later on the permeability assay with the same cell line. Cells were cultured in EMEM supplemented with 20% fetal bovine serum, 100 μ g/mL of penicillin-streptomycin and 0.25 μ g/mL amphotericin-B. 5×10^4 cells were seeded in each well (passages between 15 and 25) in a 24-well cell culture plate (Nunc, Kamstrupvej, Denmark). Experiments were performed for 24 h after the treatment. The cells were incubated under sterile conditions in a humidified atmosphere at 95%, 37°C and 5% CO₂.

Resazurin assay

Different concentrations of the lupeol-rich fraction at 10 μ g/mL, 20 μ g/mL, 50 μ g/mL and 100 μ g/mL were evaluated. As a positive control of viability, medium without the lupeol-rich fraction was used. Once the incubation time had elapsed, 50 μ L of resazurin solution were added, and cells were incubated for 3 h at 37°C and 5% CO₂. Resorufin formation by cellular metabolic activity was determined in a CLARIOstar[®] Plus plate reader (BMG LABTECH, Germany) determining fluorescence (excitation at 560 nm and emission at 590 nm). The results were obtained with the MARS[®] version 3.30 software (BMG LABTECH, Germany). The percentage of cellular cytotoxicity was determined (equation 2), considering the untreated cells as a positive control (0% cytotoxicity):

$$\text{Cytotoxicity (\%)} = (F_{\text{trat}} - F_{\text{b}}) / (F_{\text{cont}} - F_{\text{b}}) \times 100 \text{ (equation 2)}$$

Where F_{trat} is the treatment fluorescence, F_{b} is the blank fluorescence, and F_{cont} is the control fluorescence. Samples were analyzed in triplicates.

Lupeol-rich fraction encapsulation

Preparation of the polymeric solutions

The polymeric solution based on HDPAF/PEO was prepared at a solid concentration of 10% (w:w) in a polymeric ratios 1:1 in 10% (v/v) hydroalcoholic solution and with 1% of TEGO SML, as a surfactant. The solution was homogenized with magnetic stirring at 500 rpm. Then, 4 mg of the fraction of *C. uvifera* extract were dissolved in 1 mL of ethanol, added to both polymeric mixtures and homogenized in the vortex 1,500 rpm for 15 min.

Obtaining nanofibers by electrospinning

Previous solutions were processed in a Fluidnatek[®] model LE-10 equipment (Bioinicia S.L., Valencia, Spain). The parameters used were: voltage between 15–18 kV, flow rate between 60–100 μ L/h, distance from the injector to the collector between 14–18 cm, and needle inner diameter of 0.09 mm. Neat polymeric solutions were also processed as control samples.

Morphological characterization

The nanofibers morphology was characterized by scanning electron microscopy (SEM) using a SEM Hitachi S-4800 (Hitachi High Technologies Corporation, Tokyo, Japan). Samples were sputtered with a gold-palladium coating for 2 min, and SEM micrographs were taken at 10 kV. The size distribution of the structures was determined measuring at least 100 measurements per sample.

In vitro permeability test of the lupeol-rich fraction of *C. uvifera* loaded on nanofibers

The human colon adenocarcinoma cell line (Caco-2) was used to evaluate the lupeol-rich fraction permeability. These cells were cultured as explained in previous section. After 21 days, the monolayer integrity was checked by measuring the trans-epithelial electrical resistance [TEER ($\Omega \cdot \text{cm}^2$)] with a Millicell-ERS-2 volt-ohm-meter (Merck-Millipore, Darmstadt, Germany). The apparent permeability of loaded lupeol-rich fraction loaded in electrospun nanofibers was evaluated at a concentration of 20 $\mu\text{g/mL}$ of the lupeol-rich fraction and compared with the pure fraction at the same concentration as a control. Samples were analyzed in triplicates.

Apparent permeability (P_{app}) coefficient (expressed in cm/s) was calculated according to equation 3:

$$P_{\text{app}} = [V / (A \times T)] (d_r / d_d) \text{ (equation 3)}$$

Where V is the volume (mL) of the receptor compartment, A is the area (cm^2) of the Transwell membrane, T is the time (s), d_r is the concentration of lupeol in the receptor compartment, and d_d is the concentration of lupeol in the donor compartment, both expressed in (ng/mL).

Statistical analysis

Results showed in this work are the average and standard deviation of at least three replicates. The data were analyzed by applying a one-way analysis of variance (ANOVA) followed by a Tukey mean comparison test ($P \leq 0.05$). STATISTICA software version 10 (StatSoft, Inc., Tulsa, OK, USA) was used.

Results

Fractionation of the extract

The *C. uvifera* extract was fractionated by means of a chromatographic column in a total of 9 fractions. The composition of the different fractions eluted from the column was preliminary studied by TLC based on the comparison with the pure compounds, i.e., lupeol and α -amirin. In [Figure 1](#), it shows the TLC signals of lupeol and α -amirin standards and their comparison with fractions 5 and 6. Based on the similarity in signals and color intensity of the lupeol standard with fraction 6 as shown in [Figure 1](#), it is possible to preliminarily ascertain that fraction 6 showed the highest abundance of lupeol.

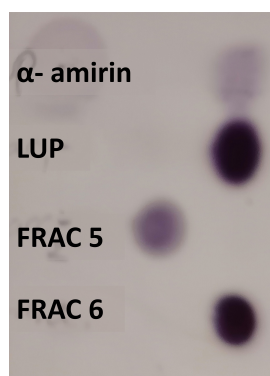


Figure 1. Preliminary identification of α -amirin and lupeol in the collected volume of the fractions 5 and 6 of the hexanic extract of *C. uvifera* by TLC. LUP: lupeol; FRAC: fraction

After fractionation, fraction 6 was subjected to solvent evaporation to concentrate the solid extract. During this process, the formation of small needles was observed.

Identification of lupeol by ATR-FTIR

Identification of lupeol in fraction 6 was made by comparison of the ATR-FTIR spectrum of fraction 6 with the spectrum of lupeol standard. The ATR-FTIR spectrum of the lupeol standard, shown in Figure 2A, presented characteristic bands at ca. 3,280 cm^{-1} and 1,043 cm^{-1} ascribed to O-H bond vibrations, ca. 2,931 and 2,872 cm^{-1} ascribed to the C-H bond in alkanes, ca. 1,640 cm^{-1} ascribed to the stretching vibration of the C=C bond, ca. 1,450 cm^{-1} ascribed to the bending vibration of the C-H bond in the cyclohexyl group, ca. 894 cm^{-1} related to the bending vibrations of the C=C-H bond.

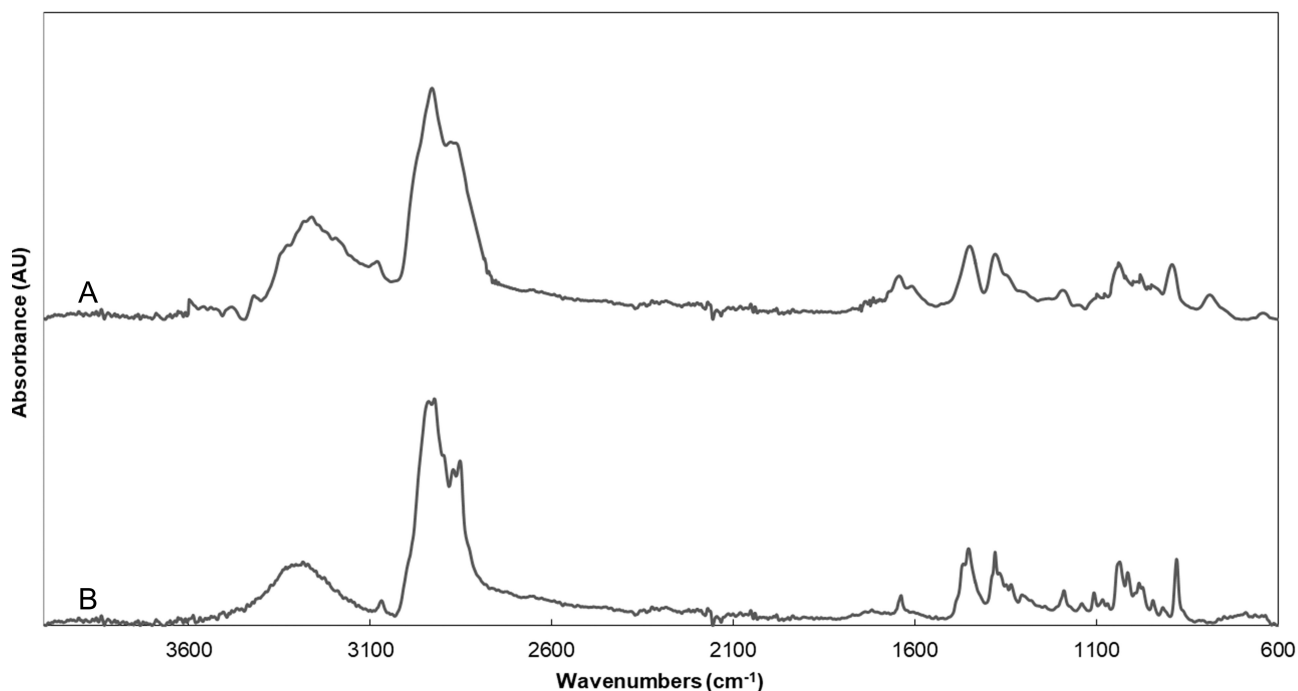


Figure 2. ATR-FTIR spectra of A: lupeol standard; B: fraction 6 of *C. uvifera* leaf extract

According to ATR-FTIR spectrum of fraction 6 shown in Figure 2B, it showed the main characteristic peaks of pure lupeol, confirming the abundance of this molecule in this fraction.

Identification of lupeol by NMR

NMR analysis was performed to elucidate the structural bonds for the identification of lupeol in fraction 6. In Figure 3A, it shows the NMR-1H one-dimensional spectrum of the lupeol compound ($\text{C}_{30}\text{H}_{50}\text{O}$). The hydrogen deficiency index (HDI) was determined obtaining a value of 6; which indicates the possible presence of double bonds. Proton signals were obtained with displacement at δ 0.768, 0.808, 0.924, 0.948, 1.009, and 1.367 ppm, a sextuplet with signals at δ 1.862, 1.879, 1.893, 1.902, 1.916, 1.933 ppm, which could correspond to the cyclic alkanes present in the structure of lupeol. On the other hand, the signals corresponding to the carbonyl group were identified with a quintuplet at δ 2.338, 2.357, 2.367, 2.375, 2.385 ppm. The doublet at δ 4.671 ppm could correspond to the shift of olefinic hydrogen bound to C-29. A singlet (δ 4.9 ppm) was also observed, which could correspond to the H of the OH group of the lupeol molecule located at C-3 (Figure 3A). In relation to the analysis of fraction 6 (Figure 3B), the presence of lupeol was confirmed by studying the one-dimensional NMR of 1H spectrum. The displacements observed in the spectrum of the fraction showed analogous signals to those obtained in the spectrum of the lupeol standard. Displacement signals were observed at δ 0.759, 0.786, 0.826, 0.942, 0.966, 1.027, 1.251, 1.679 ppm, the cyclic alkanes at δ 1.879, 1.897, 1.919, 1.934, 1.951 ppm, the presence of the carbonyl group at δ 2.384 ppm, considering a correlation between both spectra.

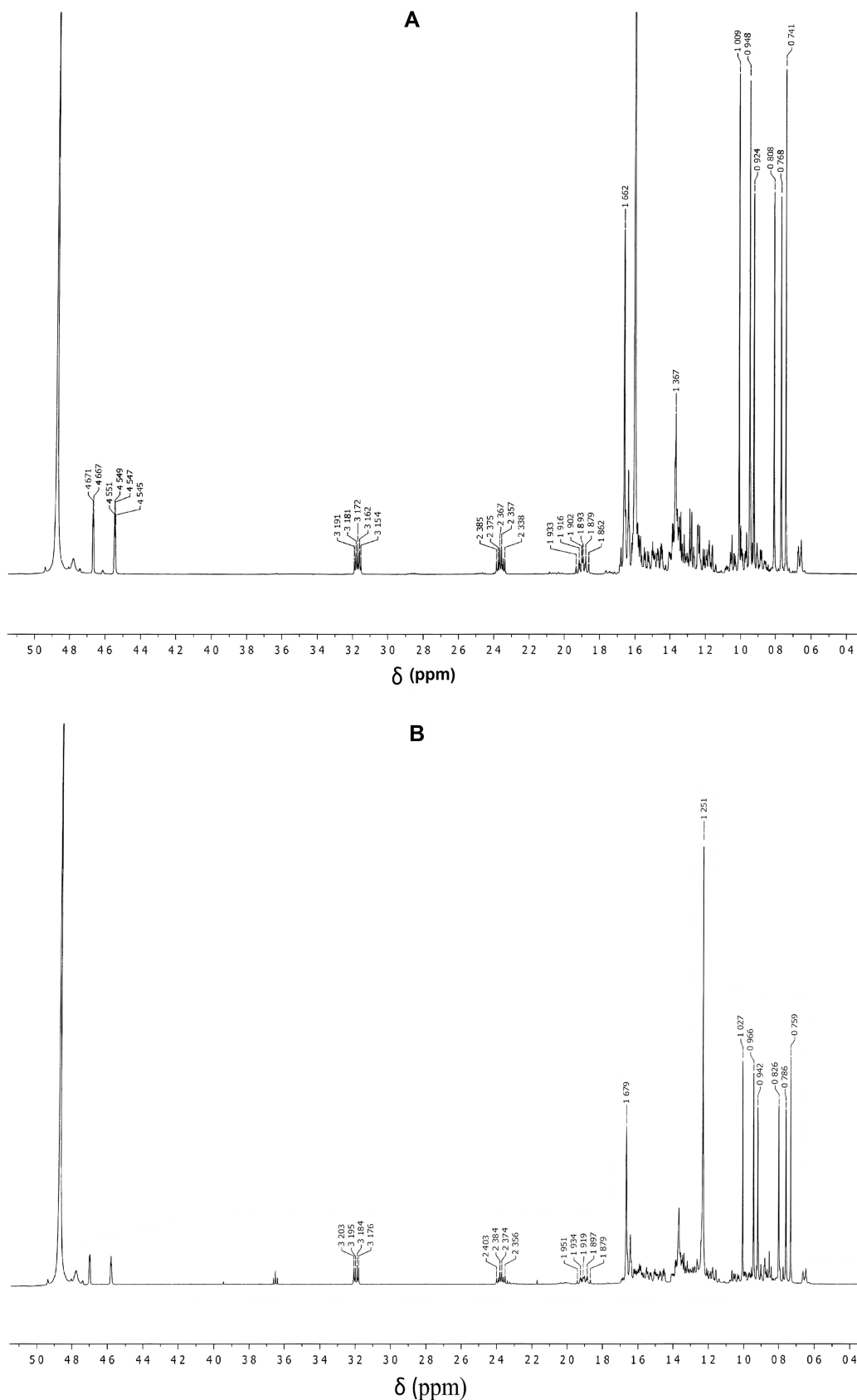


Figure 3. One-dimensional NMR-1H spectra of A: lupeol standard ($C_{30}H_{50}O$); B: fraction 6 of *C. uvifera* leaf extract

Identification and quantification of lupeol in fraction 6 by LC-MS

The LC-MS analysis allowed the identification and quantification of lupeol in fraction 6. Based on its reference standard, lupeol presented a retention time of 2.79 min. As shown in Figure 4, same retention time was observed also for fraction 6, confirming the presence of lupeol in this fraction. In addition, mass

spectrum of fraction 6 is in agreement with the mass spectrum of lupeol standard. According to the calibration curve, the abundance of lupeol in fraction 6 of the *C. uvifera* leaf extract was 0.77 mg per gram of dried fraction 6 (77%).

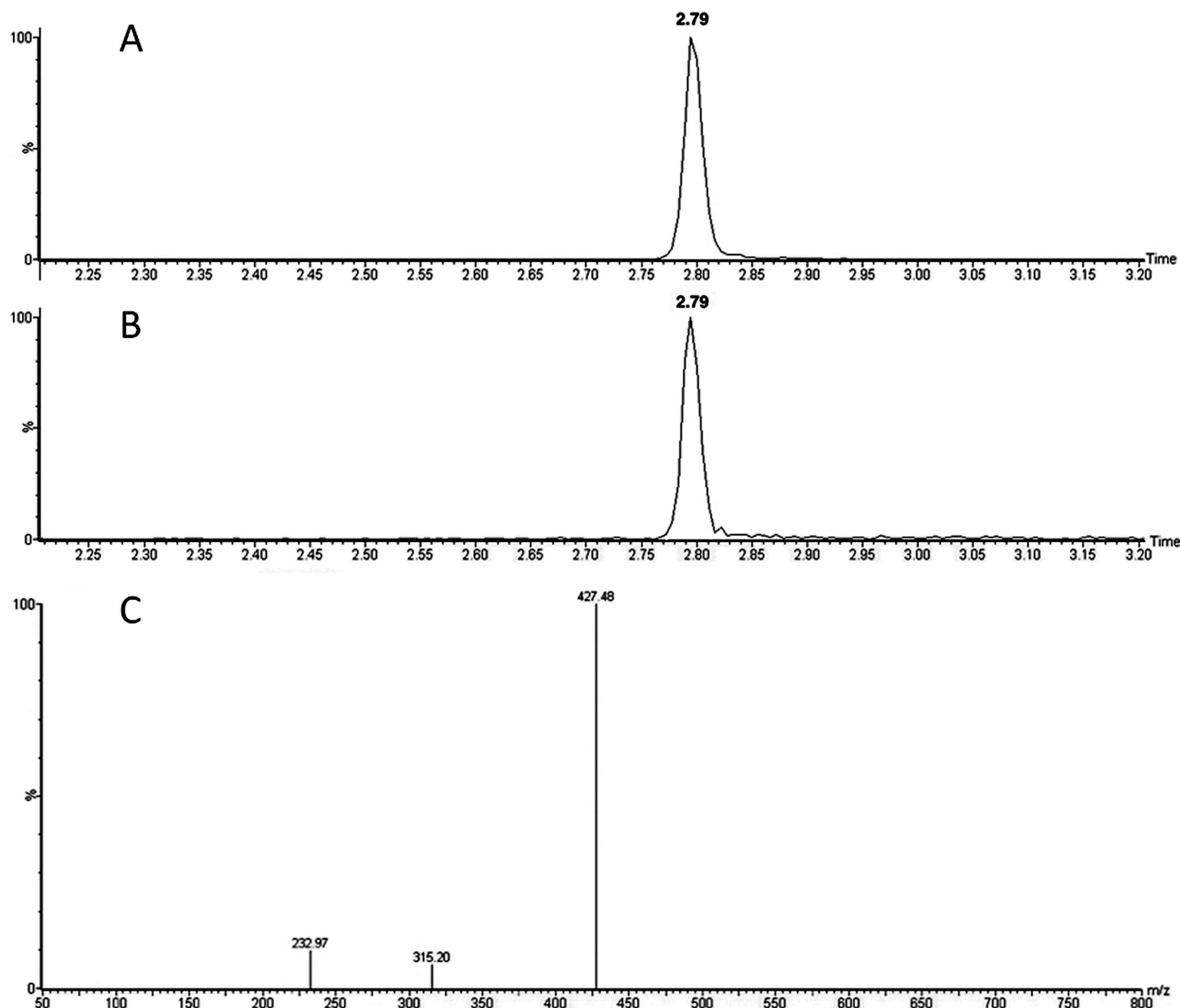


Figure 4. A: chromatograms of the lupeol standard; B: chromatogram of fraction 6; C: mass spectra of lupeol standard at 1 ppm

Determination of antioxidant capacity

The analysis of the free radical scavenging capacity DPPH revealed that the hexane extract of *C. uvifera* leaves presented a $24.6\% \pm 0.6\%$ inhibition of the DPPH radical. This result is in agreement with the result reported for the fruit pulp of *C. uvifera* with the same method, i.e. 22.8% of DPPH inhibition [13]. However, the inhibition of the DPPH radical decreased to a $7.3\% \pm 0.1\%$ for the fraction 6. Since fraction 6 has a higher concentration of lupeol than the extract, its antioxidant activity is lower.

Cytotoxicity of the lupeol-rich fraction

This assay was performed to determine the non-toxic concentrations range of fraction 6 to perform later on the permeability test. According to the results shown in Figure 5, concentrations of fraction 6 up to 50 $\mu\text{g}/\text{mL}$ did not provoke a decrease on cell viability. It is important to note that values slightly over 100% obtained at 10 $\mu\text{g}/\text{mL}$ and 20 $\mu\text{g}/\text{mL}$ were probably due to cell growth during the assay. However, 10% decrease in the viability of the cells was observed at 50 $\mu\text{g}/\text{mL}$, despite this decrease was not statistically significant. In contrast, a significant decrease of a 39% in the percentage of cell viability was observed when applying 100 $\mu\text{g}/\text{mL}$ of fraction 6 ($P \leq 0.05$).

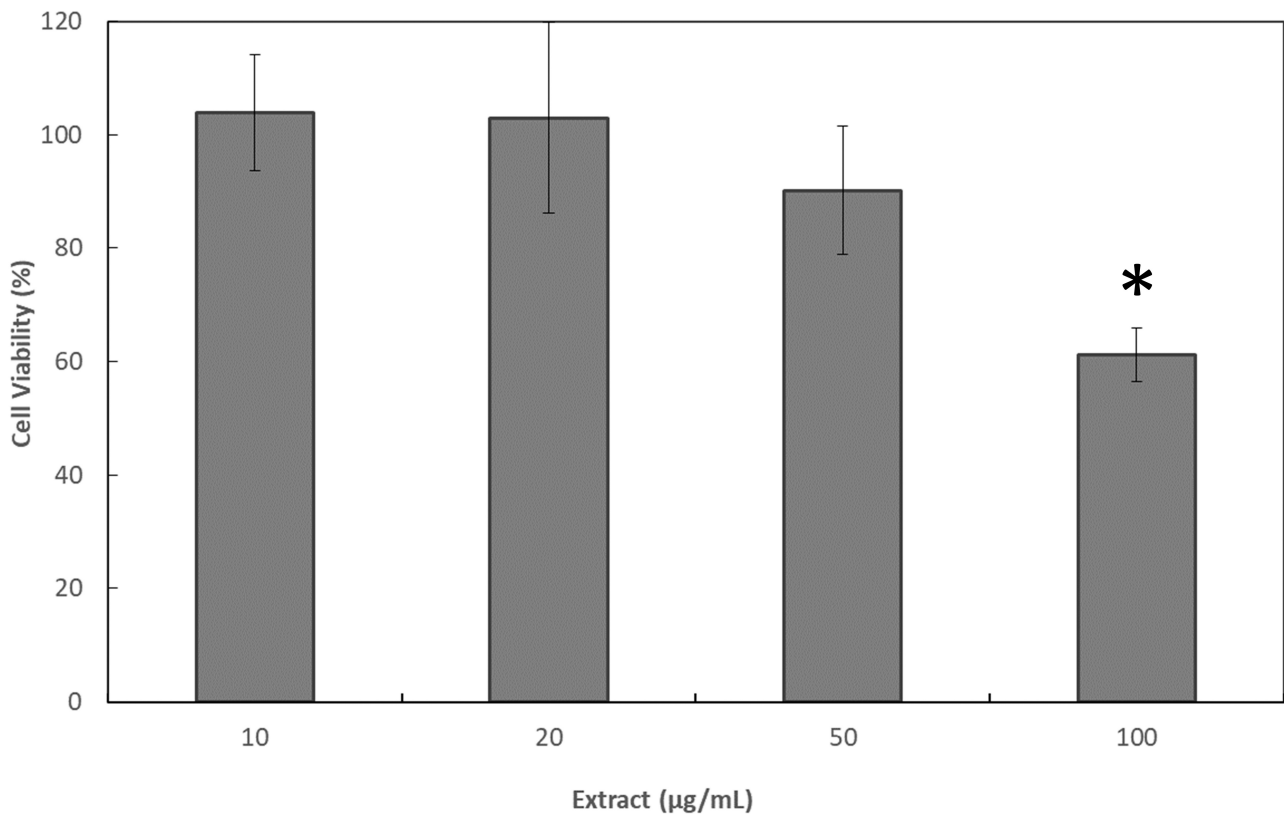


Figure 5. Cell viability 24 h after the application of treatments with fraction 6 of the *C. uvifera* hexane extract in Caco-2 cells by the resazurin assay. * Significant differences among the results ($P \leq 0.05$)

These results were also corroborated by analyzing the cell morphology by optical microscopy (Figure 6). Important changes in cells morphology were observed in Figure 6a to Figure 6d, which were directly proportional to the increase of the concentration of fraction 6, and especially significant when applying the highest concentration of 100 µg/mL of fraction 6. The Figure 6a shows the typical appearance of a Caco-2 cell monolayer, confirming that the concentration used of fraction 6 did not have a significant effect on the cells. However, in Figure 6b and Figure 6c, stress signs were detected. Some cells started losing their adherence to the substrate due to the breakage of adhesion proteins present on the membranes. In Figure 6d, signs of apoptosis were detected including fragmentation and condensation of the cells with preservation of their organelles, to finally observe the breaking up of the cells into membrane-bound apoptotic bodies. However, this apoptosis hypothesis should be proved in further studies.

Lupeol-rich fraction encapsulation into electrospun nanofibers

Electrospun nanofibers were obtained through the electrospinning process as shown in Figure 7. Neat polymeric mixtures produced homogeneous and continuous nanofibers with a rough surface as shown in Figure 7a, with an average fiber diameter of $248 \text{ nm} \pm 46 \text{ nm}$. When incorporating the fraction into the solution, no significant differences were observed in fiber diameter, since the average size for the nanofibers encapsulating the fraction was $254 \text{ nm} \pm 57 \text{ nm}$.

Identification by FTIR-ATR of lupeol-rich fraction encapsulated in nanofibers

In Figure 8, it shows the comparison of the spectra of the HDPAF/PEO electrospun nanofibers with and without fraction 6. Band assignment for the lupeol-rich fraction was already analyzed in section "Identification of lupeol by ATR-FTIR".

In the spectrum of the HDPAF/PEO nanofibers, intense signals were observed, the vibration at $2,281 \text{ cm}^{-1}$ corresponding to an asymmetric stretching of the C-H bonds of CH_2 , the vibration at $1,093 \text{ cm}^{-1}$ associated to the stretching vibration of the C-O bonds, both signals are related to the presence of PEO, as it has been reported by Abdelrazek et al. [14] for pure PEO. The HDPAF were identified with the vibration at $1,670\text{--}1,645 \text{ cm}^{-1}$ associated to the particular β -hydroxy aldehyde stretching of the C=O bond characteristic

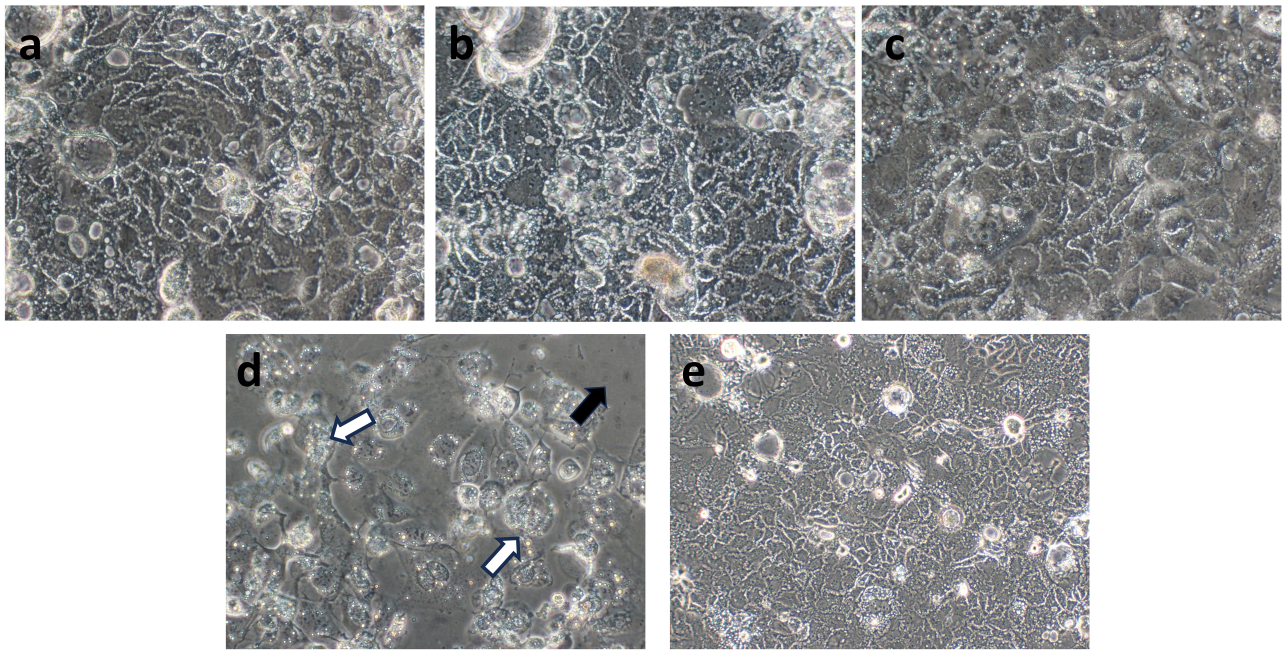


Figure 6. Representative phase contrast microscope images of Caco-2 cell morphology applying different concentrations of fraction 6 of the *C. uvifera* extract. a: 10 µg/mL; b: 20 µg/mL; c: 50 µg/mL; d: 100 µg/mL; e: positive control (20× magnification). Black arrow: many cells detached from the substrate due to the breaking up of adhesion proteins; white arrows: remaining cells showed the clear signs of apoptotic stress

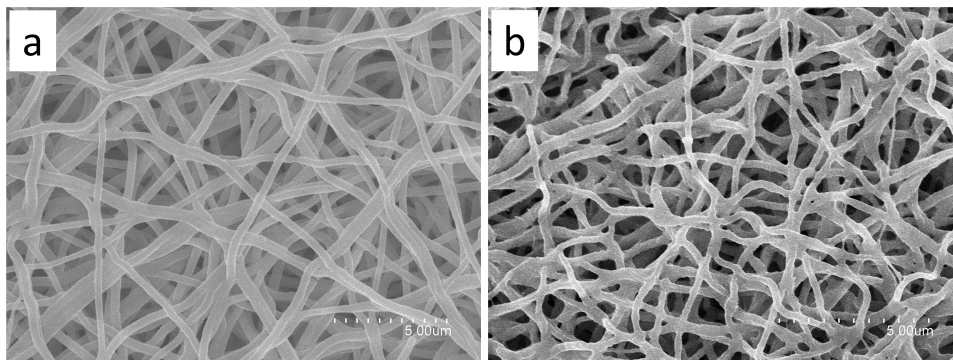


Figure 7. SEM images of nanofibers. a: neat HDPAF/PEO fibers; b: lupeol-rich fraction loaded in HDPAF/PEO fibers

of the structure of agave fructans signals and an intense broadband between 3,000–3,500 cm^{-1} , related to the C-H bond stretching, and O-H bond stretching characteristic of the hydroxyl groups. Similar characteristic bands were reported by Ramos-Hernández et al. (2018) [8] for agave fructans processed by electrospinning.

The nanofibers with the encapsulated fraction showed the characteristic bands of HDPAF and PEO. Regarding the characteristic bands of the fraction, it was possible to detect the band at 1,680–1,620 cm^{-1} assigned to C=C bonds, characteristic of the lupeol molecule. The intense band of the fraction around 2,900 cm^{-1} , which is associated with the presence of C-H bonds could not be detected in the fraction-loaded nanofibers, since this band remained hindered below the signal of the neat polymers.

Lupeol permeability of *C. uvifera* extract

The Caco-2 cells permeability of the pure fraction of the *C. uvifera* extract was compared to the permeability of the fraction of the *C. uvifera* extract encapsulated in HDPAF/PEO electrospun nanofibers. This test was performed at 20 µg of fraction/mL. Experimental apparent permeability coefficients (P_{app} , cm/s) were calculated for the time-dependent *in vitro* absorption from the apical side of the Caco-2 monolayer to the basal side of the Caco-2 monolayer.

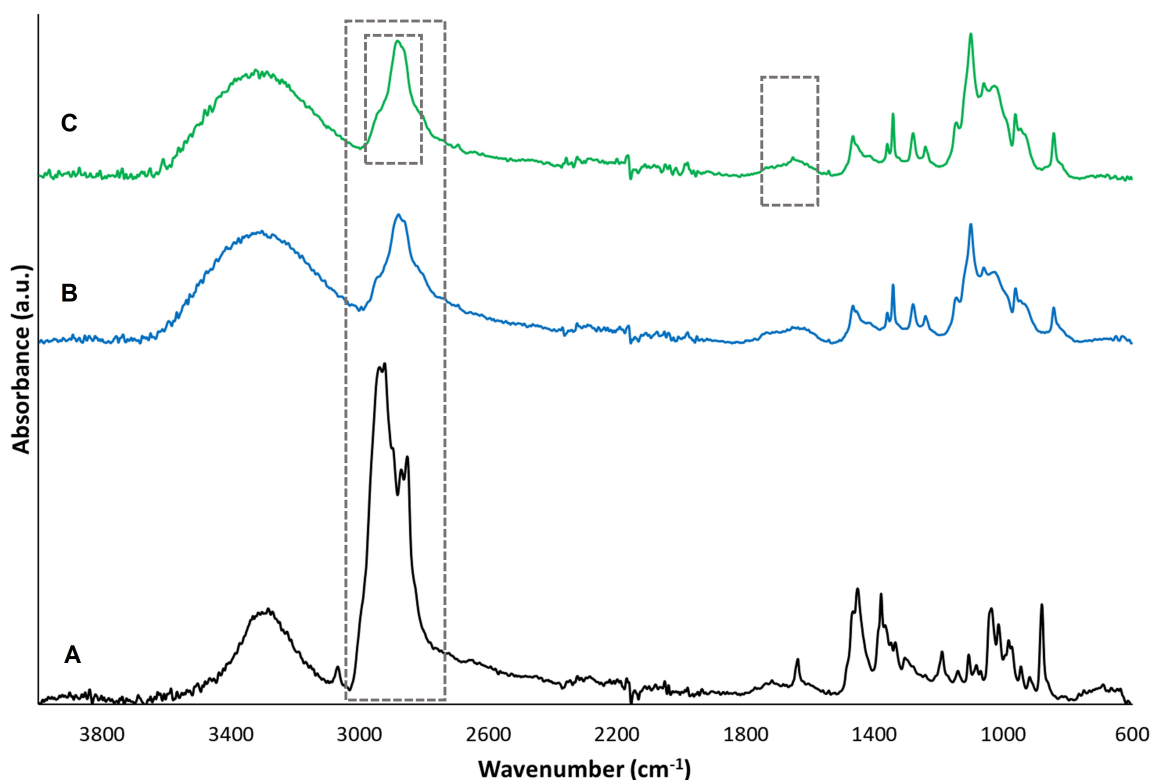


Figure 8. A: comparison of the ATR-FTIR spectra of the neat fraction; B: the neat nanofibers; C: the fraction encapsulated in the nanofibers

The results of Table 1 indicate that, 15 min after the start of the assay, the electrospun nanofibers loaded with fraction 6 presented increased lupeol permeability in comparison to the pure fraction, which did not present a response at this time. This increase in permeability may be related to the smaller drug size inside the nanofibers.

Table 1. Comparison of the P_{app} values for the HDPAG/PEO nanofibers-loaded with the fraction and the neat fraction with permeability response at 15 minutes

Sample	$P_{app} \times 10^8$ (cm/s)
HDPAG/PEO nanofibers-loaded with fraction 6	1.48 ± 0.01
Fraction 6	ND

ND: not detectable

Discussion

According to the obtained results, the column chromatography technique proved to be a viable technique that allows the effective purification of lupeol contained in the hexane extract of *C. uvifera* leaves. The similarity in TLC signals and color intensity of the lupeol standard with fraction 6 as shown in Figure 1, permitted to preliminarily ascertain that fraction 6 showed the highest abundance of lupeol of the total 9 fractions studied. Additionally, the presence of small needles after solvent evaporation of fraction 6 also evidenced the presence of lupeol, observation that agrees with Corrêa et al. (2009) [15], who also described the presence of needle crystals when isolating lupeol from the leaves of *Garcinia brasiliensis*.

The presence of lupeol in the purified fraction was also proved by ATR-FTIR as shown in Figure 2A, where the lupeol-rich fraction presented the main characteristic peaks of pure lupeol, confirming the abundance of this molecule in fraction 6. In addition, same characteristic bands were reported by Cîntă-Pînzaru et al. (2012) [16] for lupeol standard when comparing it with the spectra of triterpenes extract from *Betulaceae* birch bark. Dehelean et al. (2007) [17] also reported similar characteristic bands for pure lupeol.

NMR results shown in Figure 3 also confirmed the presence of lupeol in Fraction 6 according to its structural bonds. The signals obtained are similar to those reported for the lupeol molecule isolated from

Lannea humilis, authors indicated that the NMR of ¹H spectrum revealed some proton signals at δ 0.76, 0.79, 0.84, 0.94, 0.97, 1.00 and 1.65. A sextet of a proton was also observed at δ 2.37. The proton signal of carbinol was shown as a multiple at δ 3.2 and two proton signals at δ 4.50 and δ 4.70 characteristics of two similar protons [18].

By means of mass spectra obtained by LC-MS analysis shown in Figure 4, the presence of lupeol in fraction 6 was also confirmed. This results was also in agreement with the mass spectrum reported by Cîntă-Pînzaru et al. (2012) [16] for lupeol when extracting it from *Betulaceae* birch bark. Quantification resulted in 0.77 mg of lupeol per gram of dried fraction 6, results that confirms the abundance of lupeol in this fraction. It would be interesting in further studies to analyze the composition of the other 33% of fraction 6, since these compounds could be also responsible of the bioactive properties of this fraction together with lupeol.

However, by means of the purification performed to the extract, most of its antioxidant activity was lost in comparison to the fraction 6. This could be explained since pure lupeol exhibits a low antioxidant activity, corresponding to a 1.4% of DPPH inhibition, which is lower than the observed for other triterpenes [19]. Thus, the antioxidant activity of the extract may be due to a synergistic effect of various compounds present in the hexane extract. The observed antioxidant activity for fraction 6, which is higher than the pure lupeol, could be due mainly to the rest of compounds that constitutes the other 33% of this fraction. This loss of antioxidant activity by purifying the extract has also been identified in other extracts such as that of the stem bark of *Ficus benghalensis* L., in which the antioxidant activity ranged from 21.4% ± 0.5% to 82.6% ± 2.4% of DPPH inhibition, observing the highest antioxidant activity for the crude extract and the lowest for the aqueous fraction [20]. These authors also attributed this variation to the combined effect of different phytochemicals present in the crude extract that were separated in the fractionation.

The cytotoxicity test performed to determine the non-toxic concentration range of fraction 6 to perform the permeability test showed that concentrations of 100 µg/mL of the lupeol-rich fraction produced a decrease in the viability of Caco-2 cells as shown in Figure 5. This characteristic of the lupeol-rich fraction was also observed by Sinha et al. [21], who reported a 50% lethal concentration (LC₅₀) of 40 µM (17 µg/mL) of lupeol on SKRC-45 (metastatic human renal cell carcinoma (RCC) cell line). The effect of lupeol on cell viability was also reported in other cell lines such as the human cervical cancer cells (HeLa), where the apoptosis induction was observed with the concentration of 15 µM (6.5 µg/mL). In mouse macrophages cell line (RAW 246.7) treated with LPS, an anti-inflammatory effect of lupeol (42.5 µg/mL) was observed [22], being in both cases the results dependent on the concentration of lupeol applied. Additionally, studies carried out on HepG2 liver carcinoma cell lines mention that lupeol has high toxicity (IC₅₀ 33 µM or 14 µg/mL) unlike the effect obtained in normal AML12 hepatocytes (IC₅₀ 49 µM or 21 µg/mL), for which lupeol has been considered as a bioselective molecule for tumor cells [6]. Phytochemical investigation of *Piper capense* fractions (PCF) led to the isolation of 11 compounds, including lupeol (0.73 mg/g of fraction). The PCF fraction, where lupeol was present, and doxorubicin (as positive control drug) revealed cytotoxic effects on all 18 cancer cell lines tested [23]. This phenomenon may be related with the apoptosis signs observed on these cells by means of optical microscopy as shown in Figure 6. This alterations in cell physiology could be related to the effect of fraction 6 on the activation of the mitochondrial-mediated apoptosis pathway, inhibiting the protein kinase B (Akt/PKB) pathway [24], suppressing epithelial growth factor receptor (EGFR)/signal transducer and activator of transcription 3 (STAT3) activity [25], and inducing mitochondrial hyperfusion [21]. It has also been reported that lupeol can also inhibit the proliferation of cancer cells by inducing the cell cycle arrest by regulating phosphoinositide 3-kinase (PI3K)/Akt and wingless-related integration site (Wnt) signaling pathways and suppressing angiogenesis [26]. Lupeol could inhibit cell migration and invasion by regulating the Ras homolog gene family member A (RhoA)-Rho-associated, coiled-coil containing protein kinase 1 (ROCK1), EGFR/matrix metalloproteinase (MMP)-9, p38/mitogen-activated protein kinase (MAPK), PI3K/Akt, and MAPK/extracellular signal-regulated kinase (ERK) signaling pathways, and by suppressing angiogenesis [27], inducing caspase-3/9 activation, increasing the release of cytochrome C and negatively regulating the expressions of the Bcl-2 and Bcl-xL proteins [2]. It has been reported that lupeol treatment in the renal carcinoma cell line (SK-RC-45) with the LC₅₀ dose of 40 µM (17.1 µg/mL) for 48 h induced eventually

apoptosis through the mechanism of mitochondrial hyperfusion [21]. However, further studies would be required to confirm this hypothesis.

Electrospun nanofibers encapsulating the lupeol-rich fraction and with an average size of 250 nm were obtained by means of the electrospinning process as shown in Figure 7. The presence of lupeol in the nanofibers was confirmed by ATR-FTIR, since it was possible to detect some of the main characteristic bands of lupeol, being the other hindered below the signal of the neat polymers.

The encapsulation of the lupeol-rich fraction isolated from *C. uvifera* in the electrospun nanofibers favored its transport through the Caco-2 cell monolayer as shown in Table 1. For instance, Sipos et al. [28] also reported an increase in drug bioavailability by the use of nanoformulations, which are known by increasing the solubility [29] and absorption across the gastrointestinal barrier [30].

In conclusion, according to the obtained results, the sea grape leaf can be considered a source for this compound with potential for use in nutraceutical or pharmaceutical applications.

Abbreviations

Akt: protein kinase B

ATR-FTIR: attenuated total reflection-Fourier transform infrared

DPPH: 2,2-diphenyl-1-picrylhydrazyl

HDPAF: high degree of polymerization agave fructans

LC-MS: liquid chromatography-mass spectrometry

NMR: nuclear magnetic resonance

PEO: polyethylene oxide

SEM: scanning electron microscopy

TLC: thin-layer chromatography

Declarations

Acknowledgments

The authors' thanks to Consejo Nacional de Ciencia y Tecnología (CONACyT, Mexico) for Carla Norma Cruz Salas scholarship granted [702624]. Cristina Prieto wants to thank the Valencian Ministry of Innovation, Universities, Science and Digital Society for her postdoctoral grant [CIAPOS/2021/45].

Author contributions

MCS: Conceptualization, Writing—review & editing, Validation, Funding. JML: Conceptualization, Writing—review & editing, Validation. CP: Conceptualization, Writing—original draft, Writing—review & editing, Validation, Supervision. JARS: Conceptualization, Writing—review & editing, Validation, Supervision, Funding. CNCS: Investigation, Writing—original draft. ZE: Investigation, Writing—original draft, Validation. All authors read and approved the submitted version.

Conflicts of interest

The authors declare that they have no conflicts of interest.

Ethical approval

Not applicable.

Consent to participate

Not applicable.

Consent to publication

Not applicable.

Availability of data and materials

Not applicable.

Funding

This study was supported by the Consejo Nacional de Ciencia y Tecnología (CONACyT, Mexico) [316948] and the CYTED thematic network [319RT0576]. The funders had no role in study design, data collection and analysis, decision to publish, or preparation of the manuscript.

Copyright

© The Author(s) 2023.

References

1. Gobo LA, Viana C, Lameira OA, de Carvalho LM. A liquid chromatography-atmospheric pressure photoionization tandem mass spectrometric (LC-APPI-MS/MS) method for the determination of triterpenoids in medicinal plant extracts. *J Mass Spectrom*. 2016;51:558–65.
2. Alam P, Al-Yousef HM, Siddiqui NA, Alhowiriny TA, Alqasoumi SI, Amina M, et al. Anticancer activity and concurrent analysis of ursolic acid, β -sitosterol and lupeol in three different *Hibiscus* species (aerial parts) by validated HPTLC method. *Saudi Pharm J*. 2018;26:1060–7.
3. Somensi LB, Costa P, Boeing T, Mariano LNB, Longo B, Magalhães CG, et al. Gastroprotective properties of lupeol-derived ester: pre-clinical evidences of lupeol-stearate as a potent antiulcer agent. *Chem Biol Interact*. 2020;321:108964.
4. Kuete V, Krusche B, Youns M, Voukeng I, Fankam AG, Tankeo S, et al. Cytotoxicity of some Cameroonian spices and selected medicinal plant extracts. *J Ethnopharmacol*. 2011;134:803–12.
5. Gangadharan C, Arthanareeswari M, Pandiyan R, Ilango K, MohanKumar R. Enhancing the bioactivity of Lupeol, isolated from *aloe vera* leaf via targeted semi - synthetic modifications of the olefinic bond. *Mater Today Proc*. 2019;14:296–301.
6. Nyaboke HO, Moraa M, Omosa LK, Mbaveng AT, Vaderament-Alexe NN, Masila V, et al. Cytotoxicity of lupeol from the stem bark of *Zanthoxylum gillettii* against multi-factorial drug resistant cancer cell lines. *Investig Med Chem Pharmacol*. 2018;1:10.
7. Ruiz-Montañez G, Ragazzo-Sánchez JA, Calderón-Santoyo M, Velázquez-de la Cruz G, Ramírez de León JA, Navarro-Ocaña A. Evaluation of extraction methods for preparative scale obtention of mangiferin and lupeol from mango peels (*Mangifera indica* L.). *Food Chem*. 2014;159:267–72.
8. Ramos-Hernández JA, Calderón-Santoyo M, Navarro-Ocaña A, Barros-Castillo JC, Ragazzo-Sánchez JA. Use of emerging technologies in the extraction of lupeol, α -amyrin and β -amyrin from sea grape (*Coccoloba uvifera* L.). *J Food Sci Technol*. 2018;55:2377–83.
9. Cruz-Salas CN, Prieto C, Calderón-Santoyo M, Lagarón JM, Ramos-Hernández JA, Ragazzo-Sánchez JA. Antimutagenic and antiproliferative activity of the *Coccoloba uvifera* L. extract loaded in nanofibers of gelatin/agave fructans elaborated by electrospinning. *Anticancer Agents Med Chem*. 2022;22:2788–98.
10. Vettorazzi A, de Cerain AL, Sanz-Serrano J, Gil AG, Azqueta A. European regulatory framework and safety assessment of food-related bioactive compounds. *Nutrients*. 2020;12:613.
11. Harvey AL. Natural products in drug discovery. *Drug Discov Today*. 2008;13:894–901.
12. Kwon HH, Yoon JY, Park SY, Min S, Kim YI, Park JY, et al. Activity-guided purification identifies lupeol, a pentacyclic triterpene, as a therapeutic agent multiple pathogenic factors of acne. *J Invest Dermatol*. 2015;135:1491–500.

13. Segura Campos MR, Ruiz Ruiz J, Chel-Guerrero L, Betancur Ancona D. *Coccoloba uvifera* (L.) (*Polygonaceae*) fruit: phytochemical screening and potential antioxidant activity. *J Chem.* 2015;2015:534954.
14. Abdelrazek EM, Abdelghany AM, Badr SI, Morsi MA. Structural, optical, morphological and thermal properties of PEO/PVP blend containing different concentrations of biosynthesized Au nanoparticles. *J Mater Res Technol.* 2018;7:419–31.
15. Corrêa RS, Coelho CP, dos Santos MH, Ellena J, Doriguetto AC. Lupeol. *Acta Crystallogr C.* 2009;65:o97–9.
16. Cîntă-Pînzaru S, Dehelean CA, Soica C, Culea M, Borcan F. Evaluation and differentiation of the *Betulaceae* birch bark species and their bioactive triterpene content using analytical FT-vibrational spectroscopy and GC-MS. *Chem Cent J.* 2012;6:67.
17. Dehelean CA, Cîntă Pînzaru S, Peev C, Şoica C, Antal DS. Characterization of birch tree leaves, buds and bark dry extracts with antitumor activity. *J Optoelectron Adv Mater.* 2007;9:783–7.
18. Achika JI, Ayo RG, Habila JD, Oyewale AO. Terpenes with antimicrobial and antioxidant activities from *Lannea Humilis* (Oliv.). *Sci African.* 2020;10:e00552.
19. Malinowska MA, Sikora E, Stalińska J, Ogonowski J, Drukała J. The effect of the new lupeol derivatives on human skin cells as potential agents in the treatment of wound healing. *Biomolecules.* 2021;11:774.
20. Raheel R, Saddiqe Z, Iram M, Afzal S. *In vitro* antimitotic, antiproliferative and antioxidant activity of stem bark extracts of *Ficus benghalensis* L. *South African J Bot.* 2017;111:248–57.
21. Sinha K, Chowdhury S, Banerjee S, Mandal B, Mandal M, Majhi S, et al. Lupeol alters viability of SK-RC-45 (renal cell carcinoma cell line) by modulating its mitochondrial dynamics. *Heliyon.* 2019;5:e02107.
22. Kallubai M, Rachamalla A, Yeggoni DP, Subramanyam R. Comparative binding mechanism of lupeol compounds with plasma proteins and its pharmacological importance. *Mol Biosyst.* 2015;11:1172–83.
23. Mbaveng AT, Wamba BEN, Bitchagno GTM, Tankeo SB, Çelik İ, Atontsa BCK, et al. Bioactivity of fractions and constituents of *Piper capense* fruits towards a broad panel of cancer cells. *J Ethnopharmacol.* 2021;271:113884.
24. Prasad S, Madan E, Nigam N, Roy P, George J, Shukla Y. Induction of apoptosis by lupeol in human epidermoid carcinoma A431 cells through regulation of mitochondrial, Akt/PKB and NF-kappaB signaling pathways. *Cancer Biol Ther.* 2009;8:1632–9.
25. Min TR, Park HJ, Ha KT, Chi GY, Choi YH, Park SH. Suppression of EGFR/STAT3 activity by lupeol contributes to the induction of the apoptosis of human non-small cell lung cancer cells. *Int J Oncol.* 2019;55:320–30.
26. Zhang L, Tu Y, He W, Peng Y, Qiu Z. A novel mechanism of hepatocellular carcinoma cell apoptosis induced by lupeol via brain-derived neurotrophic factor inhibition and glycogen synthase kinase 3 beta reactivation. *Eur J Pharmacol.* 2015;762:55–62.
27. Liu K, Zhang X, Xie L, Deng M, Chen H, Song J, et al. Lupeol and its derivatives as anticancer and anti-inflammatory agents: molecular mechanisms and therapeutic efficacy. *Pharmacol Res.* 2021;164:105373.
28. Sipos B, Csóka I, Ambrus R, Schelz Z, Zupkó I, Balogh GT, et al. Spray-dried indomethacin-loaded polymeric micelles for the improvement of intestinal drug release and permeability. *Eur J Pharm Sci.* 2022;174:106200.
29. Li Z, Xu X, Wang Y, Kong L, Han C. Carrier-free nanoplatfroms from natural plants for enhanced bioactivity. *J Adv Res.* 2022;50:159–76.
30. Babadi D, Dadashzadeh S, Osouli M, Daryabari MS, Haeri A. Nanoformulation strategies for improving intestinal permeability of drugs: a more precise look at permeability assessment methods and pharmacokinetic properties changes. *J Control Release.* 2020;321:669–709.